Meniscus Formation and Breakdown of Thin Polymer Films in Microchannels

Kahp Y. Suh, Pil Jin Yoo, and Hong H. Lee*

School of Chemical Engineering, Seoul National University, Seoul 151-742, Korea

Received October 30, 2001

ABSTRACT: We report for the first time transient behavior of the meniscus of thin polymer films (<100 nm) in microchannels. Because of film−substrate interactions, the minimum meniscus height can keep decreasing as the meniscus develops, and this meniscus-induced reduction in the film thickness can cause an instability across the channel. A simple model can explain the instability satisfactorily.

Introduction

The meniscus is a well-defined, classical phenomenon that is well described by Young's law.[1,2] However, there are only a few studies that deal with the transients associated with meniscus.[3−6] Ghatak et al.[3] reported a meniscus instability that leads to the formation of stationary fingers when an elastic film on a glass substrate is brought into the proximity of a curved glass plate. Sharma and Reiter[4,5] presented computations on the rupture of a thin liquid film due to the meniscus-induced film thinning. de Ryck[6] investigated theoretically the instability of a meniscus caused by surface tension gradient-driven flow.

Meniscus formation in thin films, unlike the bulk behavior, has a unique feature in that intermolecular interactions of long range[7−9] can play a significant role. The nonretarded interactions across the substrate−film−air system is given by[10]

$$\Delta G = -\frac{A_{\text{eff}}}{12\pi {h_0}^2} \tag{1}$$

where ΔG is the excess free energy of the layer, A_{eff} is the effective Hamaker constant for the van der Waals interactions of the film with the surrounding media, and h_0 is the initial film thickness. The thermodynamic stability of the film is directly related to the sign of the second derivative of ΔG with respect to h.[9,11−13] For example, when $\partial^2\Delta G/\partial h^2$ is negative, the film is unstable. In this case, the local film thickness decreases with the corresponding thickness increase in some other place. Small undulations of the surface should grow spontaneously, leading to spinodal dewetting.[12]

Our interest in this paper is whether the behavior of the meniscus of a thin polymer film in a microchannel is affected by the film−substrate interactions. The subject is quite intriguing as it provides useful information on the meniscus formation on a micrometer scale, which has not been explored so far. Two major factors differentiate our experiment from previous studies. One is the confinement by the small channel width, typically on the order of micrometers, and the other is the interactions at the film−substrate interface.

* To whom correspondence should be addressed. E-mail: honghlee@plaza.snu.ac.kr.

Experimental Section

To investigate the subject, we used a technique called "capillary force lithography (CFL)".[14] When an elastomeric mold such as poly(dimethylsiloxane) (PDMS) with a desired pattern is placed on a polymer surface and heated above the glass transition temperature, capillary force allows the polymer melt to fill up the void space of the channels formed between the mold and the polymer, thereby generating a meniscus within the channel. A schematic diagram of the experimental procedure is shown in Figure 1a.

We fabricated a PDMS (Sylgard 184, Dow Corning) mold that has a planar surface with recessed patterns by casting PDMS against a complementary relief structure prepared by the photolithographic method.[15] Line-and-space patterns (1 and 2 μm) with a step height of 550 nm were used in our experiment. The mold with the pattern was placed on the surface of a polymer layer spin-coated onto a silicon substrate and then heated well above the glass transition temperature of the polymer (typically 150 °C). For the polymer, we used commercial polystyrene (PS) (molecular weight = 2.3×10^5, T_g = 101 °C). A silicon wafer that was used as the substrate was cleaned by ultrasonic treatment in trichloroethylene and methanol for 5 min each and dried in nitrogen. Native oxide was not removed of the surface and thus would exist on the surface. The film thickness was measured by elipsometry. Atomic force microscopy (AFM) measurements were made with a Nanoscope IIIa (Digital Instrument), operated in a contact mode.

Results and Discussion

Figure 2 shows the AFM images of 51 nm PS film for 1 μm (Figure 2a−c) and 2 μm (Figure 2d−f) line-and-space patterns for various annealing times. The inset in each figure is the cross-sectional thickness profile of the image. In the initial stage, the polymer starts wetting the wall, and the radius of curvature (r) is not uniform along the meniscus (Figure 2a,d). As the annealing time increases, a meniscus slowly develops within the channel with the contact angle monotonically decreasing from 90° to the equilibrium value (Figure 2b,e). If we use 20, 6, and 40 mJ/m^2 for the interfacial tensions at PDMS−air, PDMS−PS, and PS−air interfaces, respectively,[16] we obtain a contact angle of 70°. From the cross-sectional image, we obtain an equilibrium contact angle of 73° for the film (Figure 2c), which is slightly larger than the value predicted from Young's law. For the 2 μm pattern, however, the meniscus breaks down (Figure 2f), and eventually the mass in the channel splits into two parts.

10.1021/ma011890l CCC: $22.00
Published on Web 04/19/2002

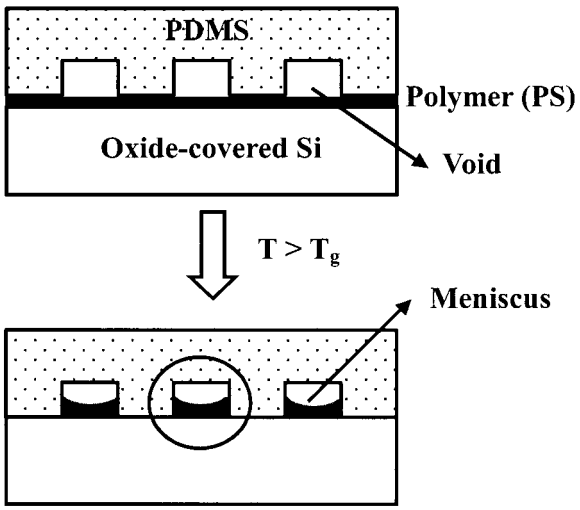

(a)

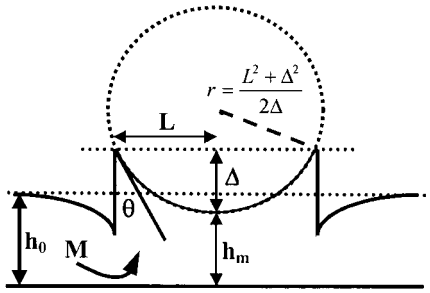

$$Vol = 2L(h_m + \Delta) - L^2[(\pi/2 - \theta)\cos^{-2}\theta - \tan\theta]$$
$$= h_0(2L) + 2M \quad \text{(Within the channel)}$$

(b)

Figure 1. (a) A schematic diagram of the experimental procedure. (b) Transient behavior of thickness profile in and near the channel in (a) (circled part).

To gain a better understanding of the meniscus formation, we utilize a simple mass balance. Referring to Figure 1b, the mass balance, when solved for h_m, yields

$$h_m = h_0 + h^* - f(\theta)L \tag{2}$$

where h^* is M/L, which is the mass transported into the channel from the regions adjacent to the channel, M, divided by the half channel width, L. Here h_m is the height of the lowest point of the meniscus, which is to be referred to as "minimum meniscus height", h_0 is the original film thickness, and $f(\theta)$ is a function solely of the contact angle θ given by $f(\theta) = (2 - \sin\theta)/(2\cos\theta) - (\pi/2 - \theta)/(2\cos^2\theta)$ that can be obtained from the simple geometric consideration given in Figure 1b. The transient can be obtained by differentiating eq 2, which gives

$$\frac{d}{dt}h_m = \frac{d}{dt}h^* - L\frac{d}{dt}f(\theta) \approx \frac{d}{dt}h^* + \frac{L}{6}\frac{d}{dt}\theta \tag{3}$$

The gradient, $df/d\theta$, is almost constant at $(-1/6)$ in the θ range of interest (70−90°) such that the factor $L/6$ appears in eq 3.

The change of the minimum meniscus height with time is due to two factors. One is the rate of mass flow from the regions adjacent to the channel (dh^*/dt in eq 3), and the other is the change due to the meniscus formation ($L/6\ d\theta/dt$). The origin of the first contribution is clear in that the thin film would wet the mold wall, and the mass in need should be supplied from somewhere else. The origin of the second contribution, on the other hand, is more involved than the first. In the initial transient, its driving force is the approach to the equilibrium contact angle, eventually reaching the meniscus height corresponding to the equilibrium. When the meniscus thickness is relatively small, however, the film−substrate interactions in the form of London force come into play. In our experiment, $\partial^2\Delta G/\partial h^2$ is negative[13] such that the meniscus can recede downward below the height corresponding to the equilibrium. In particular, this lowering of the minimum meniscus height has been observed in our experiment for thin films of thickness less than 100 nm, the thickness below which the long-range interactions take hold.[17,18]

The transients of the minimum meniscus height h_m, the height equivalent to mass flux h^*, and the contact angle θ are shown in Figure 3. The value of h_m was determined from cross-sectional AFM thickness profiles as indicated in Figure 1b and the contact angle from the relationship $\cos\theta = 2(\Delta/L)/[1 + (\Delta/L)^2]$, for which Δ was obtained from the AFM profiles. The value of h^* was calculated from eq 2.

Several notable findings emerge from the transients in Figure 3. When a stable meniscus forms as in Figure 3a for the 1 μm wide channel, the contact angle gradually decreases with time, eventually reaching the equilibrium contact angle. On the other hand, the minimum meniscus height decreases until the equilibrium contact angle is reached but then increases with time due to the mass transport from the regions adjacent to the channel. During this time, h^* that represents the mass transported keeps increasing. The finding here is that the minimum meniscus height decreases despite continuous mass supply, and only when the equilibrium contact angle is reached would the meniscus start rising. When a stable meniscus does not form as in Figure 3b for the 2 μm wide channel, on the other hand, the contact angle keeps decreasing with time even after the equilibrium contact angle is reached. The minimum meniscus height also keeps decreasing with time despite continuous mass supply as indicated by the steady increase in h^*. Further annealing (more time) leads to a new type of instability across the channel. In fact, we found that the meniscus breaks down at the time the contact angle becomes less than 70° (Figure 2f), and eventually the mass in the channel splits into two parts, one each along the two walls. The origin of this instability has to do with the film−substrate interactions or London force. If the conditions are such that the minimum meniscus height becomes sufficiently small in the process of reaching the equilibrium contact angle, the London force becomes strong enough to cause dewetting, which leads to meniscus-induced instability.

To explain the meniscus breakdown in the 2 μm channel, we use the continuity equation for a lateral flow in a thin film.[19] A unique feature in our system is that the thickness is not uniform in the channel due to the meniscus. Therefore, we write the profile for thick-

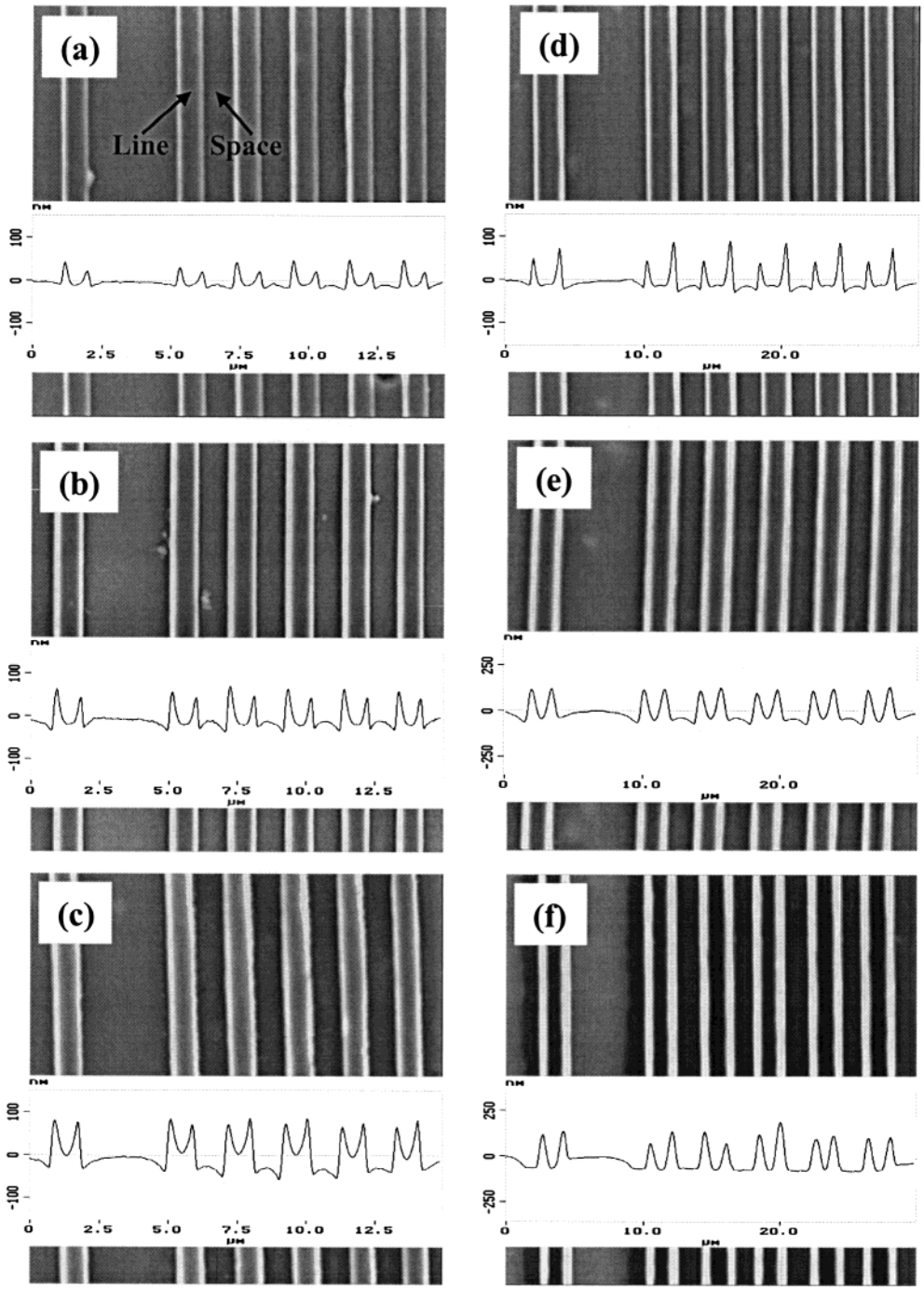

Figure 2. AFM images of transient morphologies for 51 nm PS films for various annealing times: (a) 30, (b) 80, and (c) 170 min are for 1 μm; (d) 30, (e) 80, and (f) 170 min are for 2 μm line-and-space patterns. The inset in each figure is the corresponding cross-sectional, thickness profile of the image. The scan sizes are 15 × 15 and 30 × 30 μm^2 for the 1 and 2 μm pattern, respectively. Negative thickness in the figure indicates that the point or the line in question is below the average film thickness.

ness fluctuation as follows:

$$h(x,t) = h_0 g(x) + \epsilon \cos(q_n x) \exp(t/\tau) \qquad (4)$$

where $h(x,t)$ is the local film thickness, $g(x)$ is a function that represents the meniscus curvature in the channel, x being the axis across the channel, ϵ is the perturbation amplitude, q_n is the wave vector across the channel, and τ is the characteristic relaxation time. Although $g(x)$ is dependent on x, its effect can be neglected in comparison with the exponential growth of unstable wave once the instability sets in. The equation of motion for the lateral flow in a thin film can be written from the continuity equation as follows:[19]

$$\frac{\partial}{\partial t} h(x,t) = C \frac{\partial^2}{\partial x^2} p[h(x,t)] \qquad (5)$$

where C is the constant that is responsible for the shape of the flow profile and the viscosity of the film and $p(x,t)$ is the film pressure, which can be written as

$$P = \frac{A_{\text{eff}}}{6\pi h^3} - \gamma \frac{\partial^2 h}{\partial^2 x} \qquad (6)$$

where A_{eff} is the effective Hamaker constant for the van

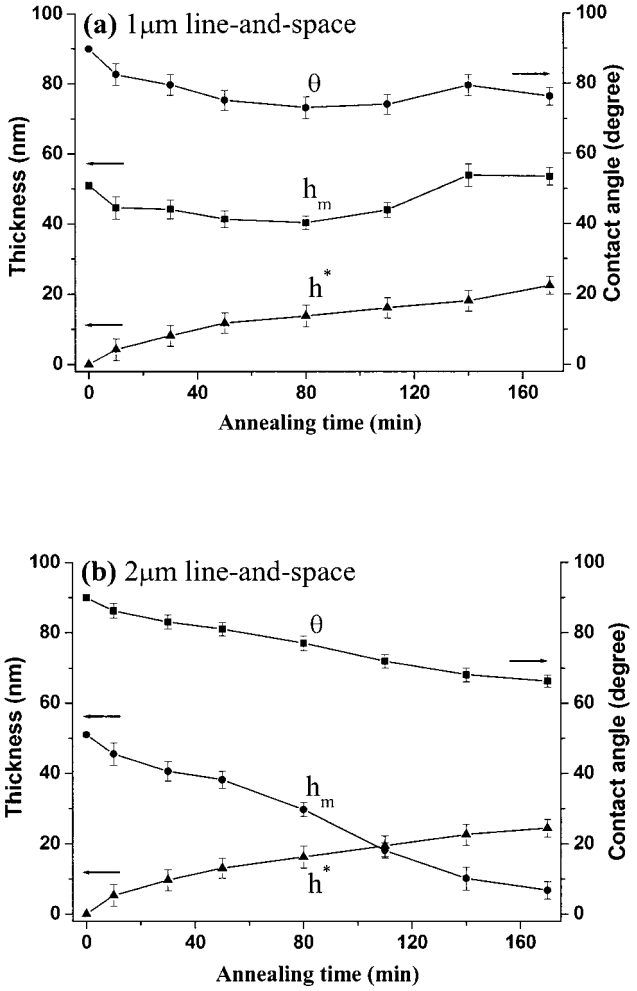

Figure 3. Transient behavior of h_m, h^*, and θ in Figure 2 as a function of annealing time.

der Waals interactions of the film with the surrounding media and γ is the surface tension of the film. Inserting eq 4 into the continuity equation and keeping only terms linear in the amplitude of the fluctuation gives

$$(C\tau)^{-1} = \frac{A_{\text{eff}}}{2\pi h_{\text{m}}^{4}} q_n^{2} - \gamma q_n^{4} \qquad (7)$$

Therefore, the time scale of instability, τ, is a function of the intermolecular interactions (A_{eff}), the minimum meniscus height (h_m), and the lateral wave vector (q_n). These parameters collectively determine whether the meniscus would be stable. For the instability, $(C\tau)^{-1}$ should be positive.

In eq 7, we assume that the intermolecular force across the film is governed by the minimum meniscus height h_m since that is the place where the force comes into play first. It is known that the wavelength and dynamics are largely determined by the minimum local thickness.[20,21]

Because of the physical constraint by PDMS mold walls, the wave across the channel should have quantized wavenumbers. Considering the mass conservation and symmetry at the center, the wave should have the form of $\cos(n\pi + n\pi x/L)$ or $(-1)^n \cos(n\pi x/L)$, which gives q_n of $n\pi/L$. In order for the PDMS walls to act as a solid boundary, the polymer should not dewet from the wall, which is true for high molecular weight (MW = 2.3×10^5) polymer as in our experiment.[22]

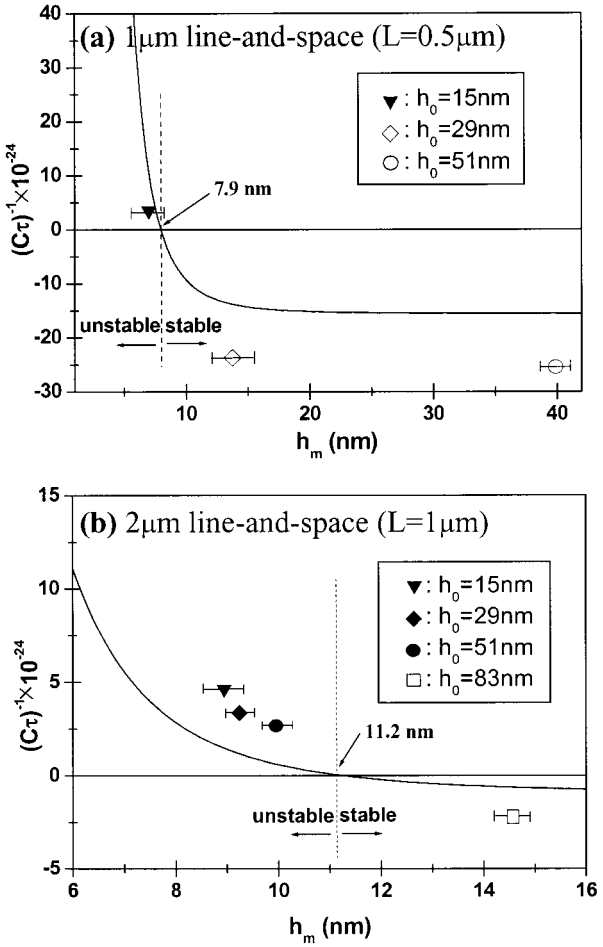

Figure 4. Plot of $(C\tau)^{-1}$ vs h_m for $n = 1$. The critical thickness for the instability is indicated by the arrow in the figure, which is the point at which the curve crosses the line, $(C\tau)^{-1} = 0$. In each figure, open symbols indicate the stable meniscus and closed symbols indicate the unstable meniscus. Note that the vertical dotted line signifies the theoretical stability crossover point. For the instability, the sign of $(C\tau)^{-1}$ and not its magnitude is of interest.

Theoretical values of $(C\tau)^{-1}$ calculated from eq 7 are shown in Figure 4 ($n = 1$) as a function of the minimum height h_m for two channel sizes. Typical parameter values for PS were used: $A_{\text{eff}} = 2.37 \times 10^{-20}$ (J)[13] and $\gamma = 40$ (mJ/m^2).[23] Also given in the figure are the experimental results. Dark symbols are used for the cases in which the instability took place; open symbols are used for the cases where a stable meniscus formed. Experimental determination of h_m is straightforward in the case of stable meniscus, the value being the minimum of the transient of h_m that can be found from the transient as in Figure 3a. In the case of unstable meniscus, the value of h_m is that corresponding to the time at which a wave starts forming, as indicated by a rise in the meniscus height at the wall. These results indicate satisfactory agreement with the stability theory.

Summary

We have shown that the experimental method presented here is an effective means by which the transient behavior of meniscus formation in a cavity can be investigated on a micrometer scale. The transients reveal that only after the equilibrium contact angle is established would the meniscus start rising. They also show that as the minimum meniscus height decreases

in the process of approaching the equilibrium contact angle and as this height becomes sufficiently small for the London force to be significant, an instability sets in across the channel that causes the meniscus to break down.

References and Notes

(1) Rowlinson, J. S.; Widom, B. In *Molecular Theory of Capillarity*; Oxford University Press: New York, 1984.
(2) Adamson, A. W.; Gast, A. P. In *Physical Chemistry of Surface*; John Wiley: New York, 1997.
(3) Ghatak, A.; Chaudhury, M. K.; Shenoy, V.; Sharma, A. *Phys. Rev. Lett.* **2000**, *85*, 4329−4332.
(4) Sharma, A.; Reiter, G. *J. Colloid Interface Sci.* **1996**, *178*, 383−399.
(5) Reiter, G.; Sharma, A. *Phys. Rev. Lett.* **2001**, *87*, 166103.
(6) de Ryck, A. *J. Colloid Interface Sci.* **1999**, *209*, 10−15.
(7) Brochard-Wyart, F.; Debregeas, G.; Fondecave, R.; Martin, P. *Macromolecules* **1997**, *30*, 1211−1213.
(8) Reiter, G. *Langmuir* **1993**, *9*, 1344−1351.
(9) Sharma, A. *Langmuir* **1993**, *9*, 861−869.
(10) Ivanov, I. B. In *Thin Liquid Films: Fundamentals and Applications*; Marcel Dekker: New York, 1988.
(11) Henn, G.; Bucknall, D. G.; Stamm, M.; Vanhoorne, P.; Jérôme R. *Macromolecules* **1996**, *29*, 4305−4313.
(12) Brochard-Wyart, F.; Daillant, J. *Can. J. Phys.* **1990**, *68*, 1084−1088.
(13) David, M. O.; Reiter, G.; Sitthaï, T.; Schultz, J. *Langmuir* **1998**, *14*, 5667−5672.
(14) Suh, K. Y.; Kim, Y. S.; Lee, H. H. *Adv. Mater.* **2001**, *13*, 1386−1389.
(15) Xia, Y.; Rogers, J. A.; Paul, K. E.; Whitesides, G. M. *Chem. Rev.* **1999**, *99*, 1823−1848.
(16) Brandrup, J.; Immergut, E. H. In *Polymer Handbook*; John Wiley: New York, 1989.
(17) Lambooy, P.; Phelan, K. C.; Haugg, O.; Krausch, G. *Phys. Rev. Lett.* **1996**, *76*, 1110−1113.
(18) Pan, Q.; Winey, K. I.; Hu, H. H.; Composto, R. J. *Langmuir* **1997**, *13*, 1758−1766.
(19) Herminghaus, S. *Phys. Rev. Lett.* **1999**, *83*, 2359−2361.
(20) Sharma, A.; Jameel, A. T. *J. Colloid Interface Sci.* **1993**, *161*, 190−208.
(21) Sharma, A.; Ruckenstein, E. *Langmuir* **1986**, *2*, 480−494.
(22) Unpublished result.
(23) Israelachvili, J. In *Intermolecular and Surface Forces*; Academic Press: New York, 1992.

MA011890L